Divertor Detachment in TCV Ohmic Plasmas

R. A. Pitts, B. P. Duval, J.-M. Moret, M. E. Fenstermacher[1], A. Loarte[2], W. H. Meyer[1], J. Mlynar, A. Refke, J. Rommers

Centre de Recherches en Physique des Plasmas
Association EURATOM - Confédération Suisse
École Polytechnique Fédérale de Lausanne, CH-1015 Lausanne, Switzerland
[1]Lawrence Livermore National Laboratory, P.O.Box 808, Livermore, California 94550, USA
[2]EFDA-CSU, Max-Planck-Institut für Plasmaphysik, D-85748 Garching, Germany

INTRODUCTION

Quantifying the effect of divertor geometry on main plasma performance and its influence on the characteristics of the divertor plasma itself constitutes an important element of current research towards an integrated solution for future reactors based on the tokamak concept. Although it is clearly preferable to perform such research in large machines [1] under conditions as close as possible to those expected in next step devices (high power, long pulse, etc), experiments in smaller, more flexible facilities can offer interesting insights into the basic phenomena occurring. Despite its small size, the possibility for plasma shape variation in TCV permits the creation of magnetic equilibria allowing the detached divertor state to be accessed, even in completely open geometries. This contribution presents selected results from the first experiments of this nature on TCV.

VARIABLE DIVERTOR GEOMETRY

In the present absence on TCV of additional heating suitable for high density operation, all experiments have been performed with ohmic heating alone and have used only D_2 gas fuelling from a single injection point in the vacuum vessel floor. Figure 1 illustrates three from a range of equilibria produced thus far and designed to investigate the effects on detachment, if any, of varying flux expansion for fixed X-point height and varying X-point height at approximately constant flux expansion. The table below describes the differences between the example equilibria of Fig. 1 in terms of magnetic geometry relevant to the divertor. Here, z_{Xpt} refers to the height of the X-point with respect to the lower divertor target tiles, L_{cmp}^{out} is the approximate magnetic connection length from outer midplane to outer divertor strike point and f_e^{out} is the flux expansion at the outer strike point (measurements on TCV are currently available only at the outer strike zone in these types of configuration). Also given are the connection lengths from X-point to

Shot	I_{p} [kA]	z_{Xpt} [m]	f_e^{out}	L_{cmp}^{out} [m]	L_{cxp}^{out} [m]
15445	340	0.57	6.8	29	21
15448	340	0.57	2.8	20	15
15521	340	0.28	2.2	13	9
15527	380	0.28	2.0	11	7

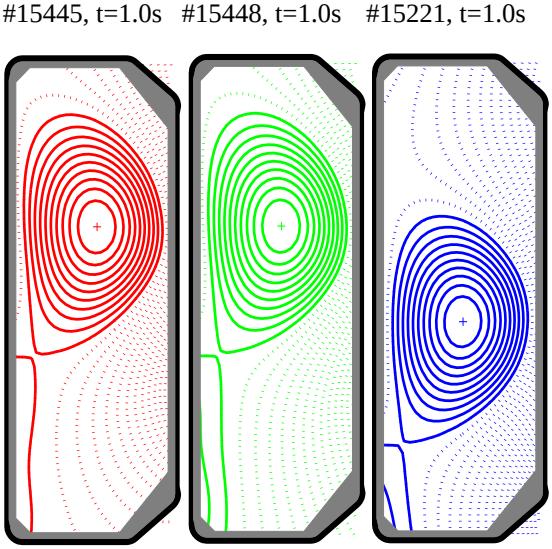

***Figure 1**: Example equilibria for detachment study illustrating large and small X-point height and low and high flux expansion at high poloidal depth. See the table alongside for more details.*

outer target, L_{cxp}^{out} for t = 1.0 s. These values highlight an important aspect of these TCV plasmas - a *substantial fraction* of L_{cmp}^{out} occurs in passing from X-point to target - the opposite of what is found in more conventional diverted equilibria. The majority of data obtained to date have been for I_p = 340 kA. Currents much lower than 300 kA result in too great a fraction of the input power being radiated inside the separatrix at high $\bar{n}_e$ to sustain the divertor plasma, whilst pushing I_p too high often leads to ohmic H-mode transitions and subsequently uncontrollable density increase. It is interesting to note, however, that configurations with low X-point height tend to remain in L-mode, even at higher current. Most experiments to date have been performed for the ion ∇B drift direction away from the X-point in the equilibria of Fig. 1.

EXPERIMENTAL OBSERVATIONS

The approach to detachment and the detachment itself are studied using density ramp discharges, frequently terminating at the density limit for the chosen value of I_p (maximum value of n_{GR} = 0.65). Figure 2 compiles a selection of plasma and divertor signals for similar ramps in main plasma density for the three equilibria of Fig. 1, corresponding to the discharge numbers listed in the accompanying table. One may immediately note the

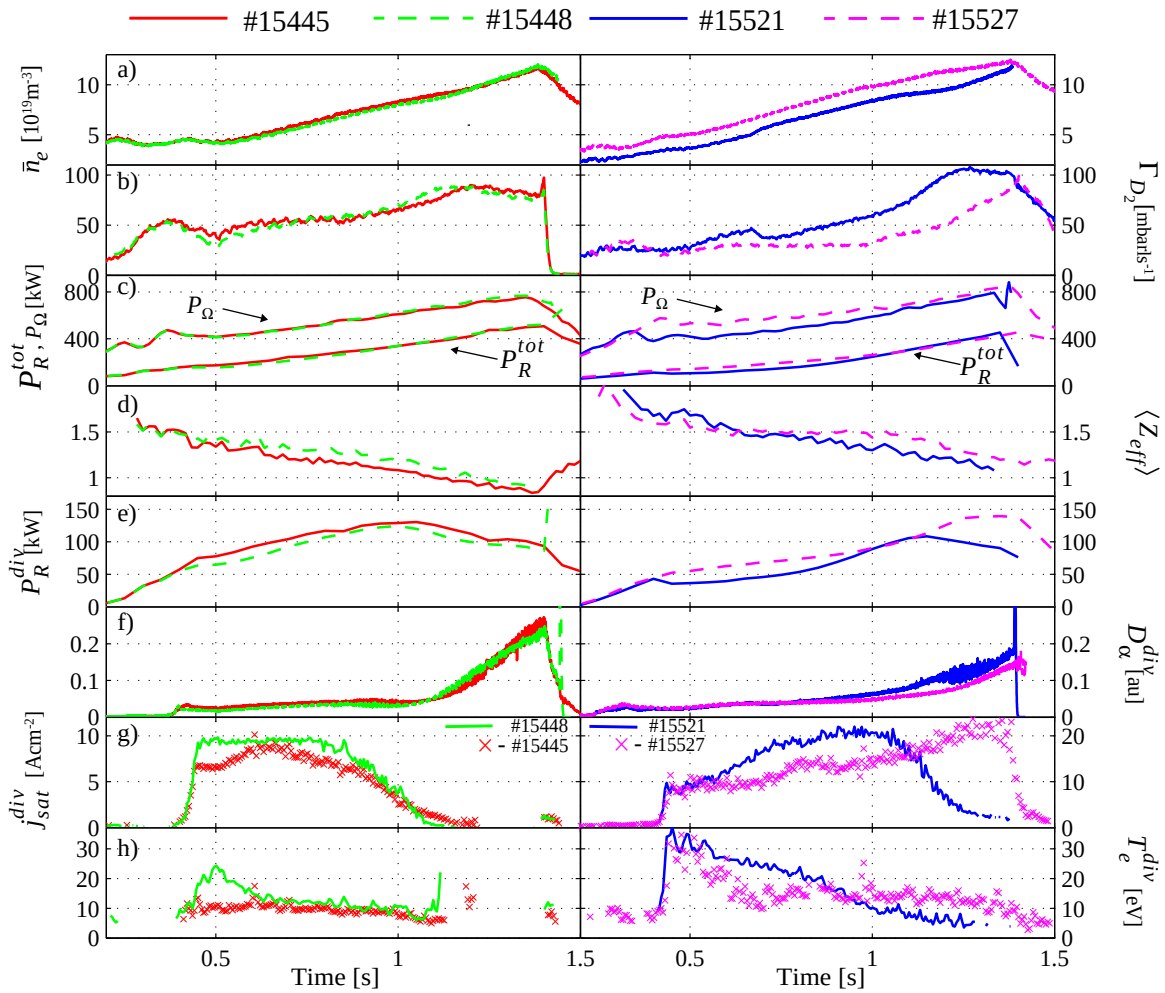

Figure 2: *Evolution of main plasma and selected divertor parameters for the discharges in the Table accompanying Fig. 1 during similar ohmic density ramps. For z_{Xpt} = 57 cm, the panels at left show both cases of f_e^{out}. Note the change in scale of the ordinate in the panels containing j_{sat}. The similarity in the D_α traces for shots #15445 and #15448 makes it difficult to discern differences if the figure is not viewed in colour.*

apparent similarity between the two discharges with identical (high) z_{Xpt} but varying flux expansion and the clear differences in behaviour when decreasing X-point height or

increasing I_p. Independent of divertor geometry, the plasma separatrix shape is approximately constant with κ_{95} and δ_{95} in the range 1.5 → 1.6 and 0.33 → 0.4 respectively with q_{95} in the range 2.2 → 3.2. Earlier studies elsewhere [2] have shown the importance of plasma wall separation in influencing bulk and divertor radiation. Attempts have been made here to minimise such differences, at least in so far as separatrix to wall gaps at the inside and outside midplane are concerned (depending on $\bar{n}_e$, I_p and z_{Xpt}, the distances typically lie in the range 2 → 3 cm). It should also be noted that the interior walls of the TCV vacuum vessel are now almost completely graphite tiled, giving ≈ 90% surface coverage.

In all cases, detachment is clearly observed at the outer strike zone as a decrease in the ion current measured near the strike point by Langmuir probes embedded in the target tiles (Fig. 2g) and an increase in the D_α emission shown, in Fig. 2f, for a chord passing almost horizontally through the divertor leg near the vessel floor. For lower z_{Xpt} , the rollover to detachment occurs at higher plasma density for fixed input power (ie fixed I_p). This is qualitatively expected since increasing L_c^{out} would be expected to facilitate the formation of parallel temperature gradients and hence low T_e in the divertor plasma. For fixed z_{Xpt} but higher I_p, detachment is observed near the strike point only at the highest densities. In all cases, detachment occurs only if $T_e^{div} \approx$ 5 eV subject to the usual uncertainty in interpretation of the Langmuir probe characteristic under high recycling conditions. The higher edge T_e at low z_{Xpt} is also reflected in higher values of $<Z_{eff}>$ for given $\bar{n}_e$ (Fig. 2d). Of note also are the low values of $<Z_{eff}>$ at high $\bar{n}_e$, even when the total radiation reaches ≈ 65% of P_Ω (Fig. 2c) and the divertor plasma detaches. This reflects both the reduced impurity source due to a decrease in divertor temperature and particle flux but also the apparent tendency for $<Z_{eff}>$ to depend principally on plasma density and radiation fraction and not the regime of divertor operation [3]. This occurs even when, at detachment, most of the radiation is concentrated at or inside the separatrix at the X-point location. The low $<Z_{eff}>$ also indicates that most of the total radiation at high $\bar{n}_e$ originates from deuterium. The traces of T_e and j_{sat} in Figs. 2g,h show that for the discharges at highest z_{Xpt}, the outer divertor plasma has already atttained the high recycling regime, even at low $\bar{n}_e$, whilst as the outer leg shortens, the divertor plasma begins life in the linear regime for the same main plasma density. Figure 3 summarises target plate measurements in terms of the integrated current to the plate surface (accounting for field line angle of incidence) and the peak divertor density, the latter not necessarily occurring in the same flux tube as $\bar{n}_e$ increases. In addition to discharges similar to those of Fig. 2, a few points available

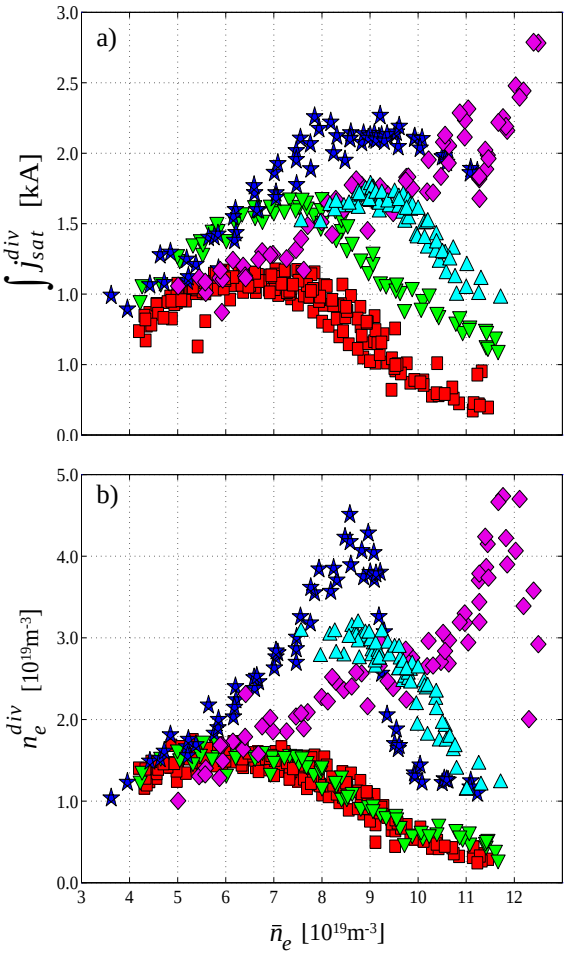

Figure 3:*Density dependence of* ***a)*** *the integrated ion current to the outer divertor target and* ***b)*** *the peak divertor density. Data are compiled from a multi-shot database. Symbols have the following meaning:* ■ z_{Xpt} = 57 *cm*, $f_e^{out} \approx 7$, ▼ z_{Xpt} = 57 *cm*, $f_e^{out} \approx 3$ ▲ z_{Xpt} = 57 *cm*, $f_e^{out} \approx 6$, ★, ◆ z_{Xpt} = 28 *cm*, $f_e^{out} \approx 2$ ■▼★, I_p = 340 kA, ◆▲, I_p = 380 kA

at high z_{Xpt} and higher I_p have also been included. For both low and high f_e^{out}, the discharges with high z_{Xpt} show the total ion current decreasing to low values at high density, behaviour typical of complete detachment. The latter is observed at higher $\bar{n}_e$ as L_c^{out} decreases or I_p increases with much higher peak densities being attained in the divertor before detachment as input power increases. At low z_{Xpt}, particularly at I_p = 380 kA, the peak divertor density behaves roughly in accordance with the standard two-point model of the SOL [4] in which $n_e^{div} \propto \bar{n}_e$ at first then $n_e^{div} \propto \bar{n}_e^3$ at high density when high recycling is attained. At lower I_p, the maximum divertor density peaks at lower $\bar{n}_e$, as would be expected for lower L_c^{out}, but the density increase with $\bar{n}_e$ is stronger than linear at lower $\bar{n}_e$.

Figure 3 highlights some interesting differences in divertor behaviour for different input power and magnetic geometry. At high z_{Xpt} and I_p =340 kA, the total integrated ion current to the outer target (Fig. 3a) is higher at low f_e^{out}, whilst the peak divertor density (Fig. 3b) appears to be independent of flux expansion (note that the peak n_e^{div} will not always occur on the same flux tube in the divertor). Given the lower values of L_c^{out} for low f_e^{out}, this is not what would be expected from the two point model if the upstream power flow is constant for given $\bar{n}_e$. Target density profiles for the two cases at four times (or values of $\bar{n}_e$) are shown in Fig. 4. The profiles are mapped to the midplane to better illustrate the effects of flux expansion - the latter clearly has a strong effect on the profile shape. Before detachment begins, there is relatively good agreement between magnetically computed strike point and the profile peak. At high f_e^{out}, detachment penetrates further into the divertor fan and there is also faint evidence for some structure in the profile itself, not seen at low f_e^{out}. Profiles of T_e^{div} are remarkably flat and in the range $10 \rightarrow 15$ eV for both flux expansion cases at all but the lowest plasma densities and of course when detachment occurs. The observations at lower I_p are not yet understood. Part of the difficulty is almost certainly associated with low power crossing the separatrix at high density. At I_p = 380 kA, Thomson scattering measurements made just inside the separatrix (at a radius corresponding to 95% of poloidal flux) show T_e there to remain roughly fixed with increasing $\bar{n}_e$, except at the very highest densities. In contrast, for I_p = 340 kA, the temperature decreases from ≈ 50 eV at low density to only ≈ 20 eV at highest $\bar{n}_e$. This is a consequence of an increasing radiation fraction (Fig. 2c) leading to lower values of upstream conducted power. Under these circumstances, it is unlikely that the condition of $T_e^{up} \gg T_e^{div}$ for electron conduction to dominate parallel heat transport is satisfied and significant convection may occur, leading to departures from the expectations of two-point modelling.

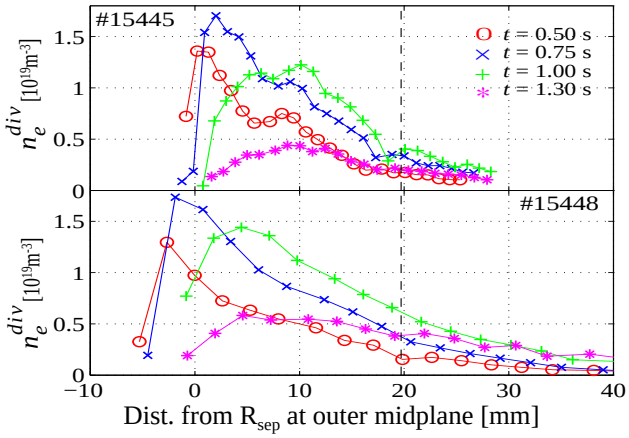

Figure 4: *Time variation of target density profile mapped to the midplane for discharges with z_{Xpt} = 57 cm and low and high f_e^{out}. The vertical dashed lines indicate the mean position of the outer wall.*

ACKNOWLEDGMENTS

This work was partly supported by the Swiss National Science Foundation.

REFERENCES

[1] L. D. Horton et al., Nuclear Fusion **39** (1999) 1
[2] A. Loarte et al., Nuclear Fusion **38** (1998) 331
[3] G. F. Matthews et al., J. Nucl. Mater. **241-243** (1997) 450
[4] C. S. Pitcher and P. C. Stangeby, Plasma Phys. Control. Fusion **39** (1997) 779